ANNALS OF GEOPHYSICS, VOL. 45, N. 2, April 2002

Aerial remote sensing hyperspectral techniques for rocky outcrops mapping

Carolina Filizzola ([1]), **Nicola Pergola** ([1]), **Stefano Pignatti** ([1]) **and Valerio Tramutoli** ([2])
([1]) *Istituto di Metodologie per l'Analisi Ambientale, CNR, Tito Scalo (PZ), Italy*
([2]) *Dipartimento di Ingegneria e Fisica dell'Ambiente, Università della Basilicata, Potenza, Italy*

Abstract
In this work the MIVIS (Multispectral Infrared and Visible Imaging Spectrometer) hyperspectral data, acquired during aerial campaigns made in 1998 over the Pollino National Park in the framework of the «Progetto Pollino», have been used to set up a supervised technique devoted to identify the presence of selected rocky outcrops. Tests have been performed over an extended area characterised by a complex orography. Within this area, serpentinite was chosen as a test-rock because it is present in isolated outcrops, distributed all over the test-area, besides subtending important problems of environmental nature as it contains asbestos. Geological information, coming from field observations or geological maps, was used to trigger the algorithms and as ground truth for its validation. Two spectral analysis techniques, SAM (Spectral Angle Mapper) and LSU (Linear Spectral Unmixing), have been applied and their results combined to automatically identify serpentinite outcrops and, in some cases, to mark their boundaries. The approach used in this work is characterised by simplicity (no atmosphere and illumination corrections were performed on MIVIS data), robustness (material of interest is identified for certainty) and intrinsic exportability (the method proposed can be applied on different geographic areas and, in theory, to identify any kind of material because no datum about atmospheric and illumination conditions is required).

Key words *hyperspectral sensor – airborne remote sensing – robust techniques – geological mapping – LSU – SAM – MIVIS – serpentinite – Pollino*

1. Introduction

It is well-known that any material reflects or emits radiation with different intensity at different wavelength, according to its own physical-chemical properties.

Theoretically, it is possible to identify different materials by analysing their characteristic spectral response (*spectral signature*, in absorption, emission or reflection) on the basis of suitable multi-spectral radiometric measures (fig. 1).

That has been easily done in controlled laboratory conditions and attested by a number of published works reporting laboratory spectral signatures of almost any material (*e.g.*, Clark *et al*., 1990; Salisbury and D'Aria, 1992).

A number of additional problems arise when surface material identification is attempted by airborne multispectral sensors. The e.m. signal leaving the investigated surface, before reaching the airborne remote sensor, is affected by spectrally selective atmospheric absorption and

Mailing address: Dr. Valerio Tramutoli, Dipartimento di Ingegneria e Fisica dell'Ambiente, Università della Basilicata, Campus di Macchia Romana, 85100 Potenza, Italy; e-mail: tramutoli@unibas.it

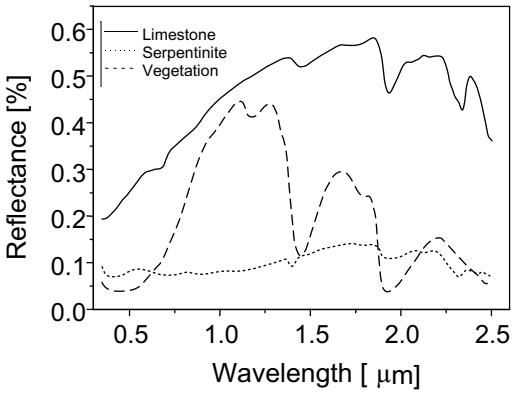

Fig. 1. Laboratory reflectance spectra of limestone, vegetation and serpentinite samples collected in the test-area using an ASD, FieldSpec FR(350-2500 nm) spectroradiometer.

scattering that corrupt the original spectral behaviour of the signal making the identification of surface properties by simple comparison with laboratory spectra misleading. Other known variable factors, not present during laboratory observations, which could affect remotely sensed spectra are mainly related to the illumination conditions (in the solar spectral range) the angles of view and surface homogeneity within the ground resolution cell.

In particular, even considering the same relative sun position and ground target characteristics, atmospheric conditions and topography greatly influence the electromagnetic signal which, leaving the ground, achieves the airborne sensor.

The presence of atmosphere, as a transmission medium through which radiation travels, modifies e.m. signals according to three main physical processes (atmosphere-radiation interaction): absorption, scattering and emission. Absorption is a spectrally selective process (mainly due to atmospheric molecules of water, carbon dioxide, ozone and oxygen) that selectively reduces the incoming e.m. signal, whereas scattering is the result of diffused multiple reflections of e.m. radiation by atmospheric gases and suspended particles which, similarly, affect the intensity (but also the spatial distribution) of the signal received by the sensor. Moreover, the atmosphere acts as a source of e.m. radiation due to its thermal state, according to Planck's law.

Topographic effects are particularly important for observations in the solar spectral range. The local landscape orientation with respect to the sensor view angle and the sun controls both the incoming sun radiation and the signal reflected toward the airborne sensor. The effects on the reflected radiances can be severe, especially in areas of high and variable relief.

Figure 2a,b shows, as an example, how the reflectance spectra of the same materials (lime-

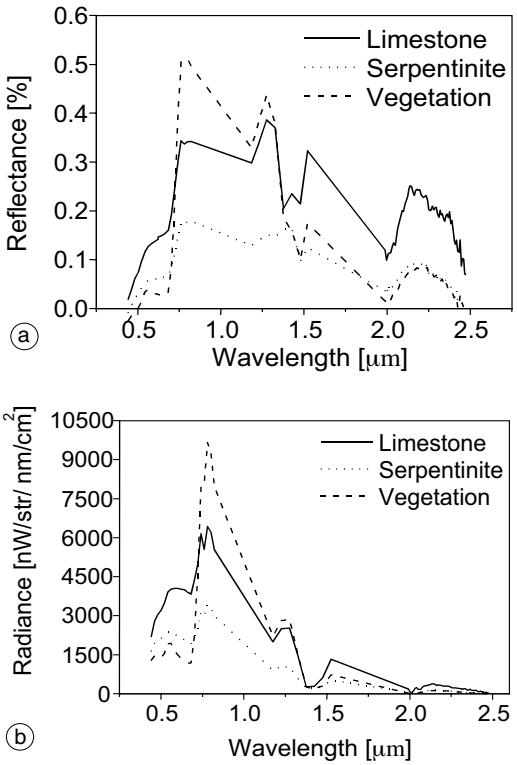

Fig. 2a,b. MIVIS spectra (not atmospherically corrected) for limestones, vegetation and serpentinites present in the test-area: a) reflectances, b) radiances at the sensor: they were used as reference for the SAM and as end-members for LSU processing steps (see text).

stone, serpentinite and vegetation) represented in fig. 1 change when retrieved from multispectral radiances acquired by an airborne sensor (MIVIS in this case) instead of controlled laboratory conditions. Comparing fig. 1 and fig. 2a, the differences between MIVIS reflectance spectra and the laboratory ones (due mainly to the presence of the atmosphere, different observational conditions and possible soil heterogeneity within the ground resolution cell) are quite evident.

2. MIVIS

Nowadays, many airborne hyperspectral sensors (AVIRIS, HYDICE, DAIS, HYMAP, etc.) are active. They are able to acquire data in a great number of narrow spectral bands which, in theory, obtain from airborne or spaceborne platforms, spectral response curves comparable with those obtained in the laboratory. Among the other hyperspectral sensors, MIVIS (Bianchi *et al*., 1994) offers a wide range of wavelengths (from the VISible to the Thermal-IR) allowing the collection of accurate spectra of any exposed material on the whole optical range.

MIVIS, operational since 1994 in the framework of the «CNR-LARA (Airborne Laboratory for Environmental Studies) Project», is a multispectral imaging system with a spectral resolution ranging between 8 and 540 nm (moving from the VIS to the TIR range) over 102 spectral bands. Its main features are reported in table I.

MIVIS data were acquired during two flights (in June and November 1998) carried out in the framework of the «Pollino Project» (Cuomo *et al*., 2001) over the whole lucan area of the Pollino National Park (fig. 3a,b).

During each flight (made at around local noon), 15 data strips (about NNW-SSE flight direction) were collected at a (relative) altitude of 3000 m and with a scan rate of 17 scans/s. According to orography and angular view, the dimensions of ground resolution cells range between 5.8 and 13.5 m.

Figure 3c points out the test-area among MIVIS strips.

3. Methodology

To identify a material by remotely sensed radiances usually they are compared with laboratory spectra (fig. 4a), after a preliminary correction step to clear atmospheric, topographic and illumination effects out of the measured signal (McArdle *et al*., 1992; Ben-Dor *et al*., 1994; Farrand *et al*., 1994; Clark *et al*., 1995; Smith and Milton, 1999). Digital elevation models are needed to correct topographic effects, while the atmospheric ones are usually evaluated by applying well-tested Radiative Transfer Models (RTM) like 6S, MODTRAN, etc. Such models simulate atmosphere-radiation interactions on the basis of information to be given on atmospheric (chemical-physical) and observational conditions at the time of the observations. Contemporary

Table I. Main characteristic of the MIVIS sensor.

FOV (Field Of View)	71.059°	
IFOV (Instantaneous FOV)	2 mrad	
Spatial resolution	6 m at 3000 m of (relative) flight height	
Swath width	4.2 km at 3000 m of (relative) flight height	
102 bands simultaneously sampled and recorded	Visible (0.43-0.83 μm)	20 bands
	Near-IR (1.15-1.55 μm)	8 bands
	Mid-IR (2.0-2.5 μm)	64 bands
	Thermal-IR (8.2-12.7 μm)	10 bands

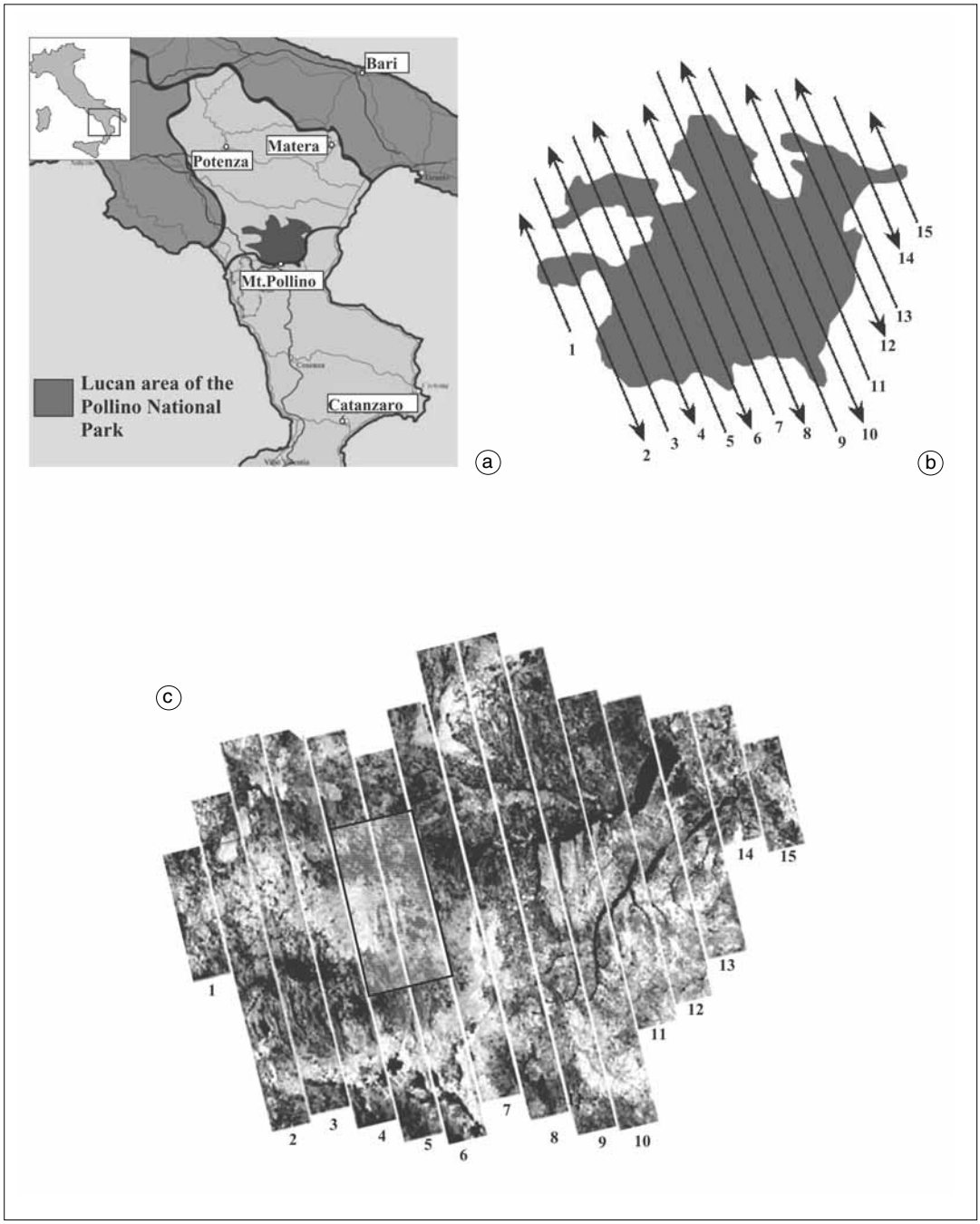

Fig. 3a-c. a) Position of lucan area of the Pollino National Park in Southern Italy; b) flight plan of MIVIS airborne hyperspectral sensor; c) MIVIS strips (the test-area is indicated by a black box).

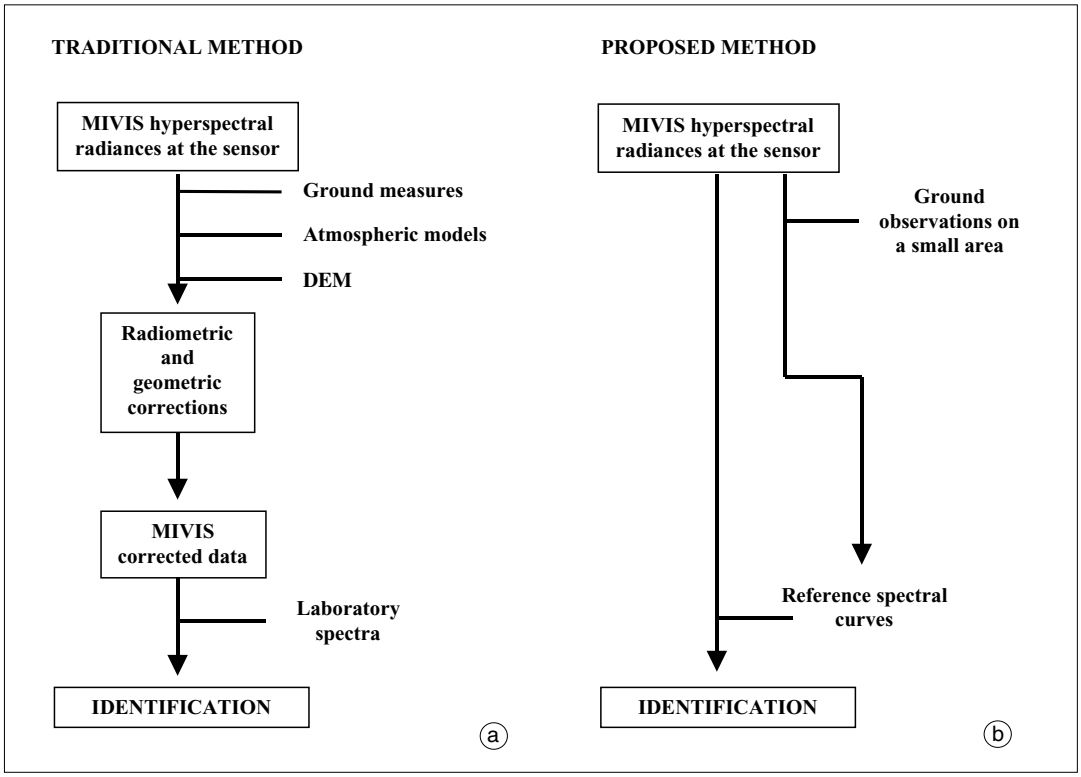

Fig. 4a,b. Material identification by hyperspectral data: flow diagrams for traditional (a) and proposed (b) methods.

ground-based measurements of atmospheric parameters (like vertical temperature and water vapour profiles, aerosol dimensional distribution and optical thickness, etc.) if available, otherwise standard atmospheric models, are required, to give the appropriate inputs to RTM codes. Whether based on punctual ground-based measurements or on standard atmospheric models, RTM codes assume an horizontally homogeneous atmosphere (physically and chemically) to perform those corrections on the whole scene. But because of the high spatial dynamic of atmospheric chemical-physical properties, the radiometric correction process will suffer errors which still remain high.

So the use of traditional radiometric correction methods can reveal poorly reliable results (large errors due to the use of not appropriate atmospheric models) and difficulties of application (requiring contemporary ground observations not always available).

In this paper, a different method (fig. 4b) is proposed to map surface materials using hyperspectral radiances at the airborne sensor and a limited set of field observations. It starts from the experimental observation that *raw* (*i.e.* not corrected for atmospheric effects) reflectance spectra (fig. 2a), notwithstanding the atmospheric effects that make them different from laboratory spectra, still distinguish different materials. This is still evident as far as radiances at the sensor are considered (fig. 2b). In this case, moreover, it is possible to see (fig. 5) how the same material, under different illumination conditions, presents

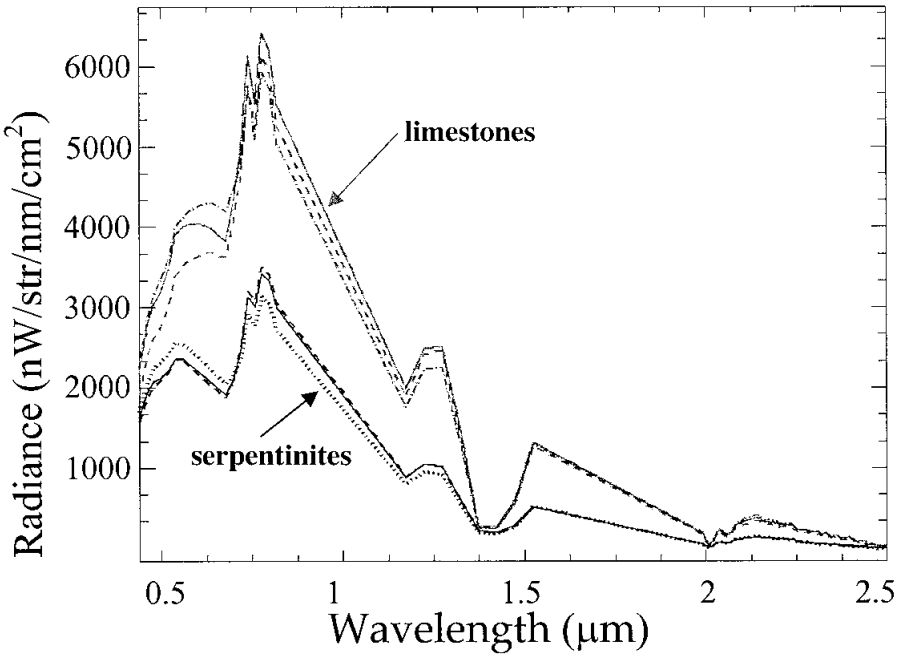

Fig. 5. MIVIS spectra (in the range 0.4-2.5 μm) for limestones and serpentinites present in the test-area under different illumination conditions.

different spectra but still with the same shape (excluding noising bands).

Starting from such considerations, spectral shapes of MIVIS radiances at the sensor (instead of MIVIS reflectance spectra obtained after correction for atmospheric effects) were considered for materials identification. To this aim, the SAM (Spectral Angle Mapper, Kruse *et al.*, 1993) supervised classification technique was implemented: it identifies surface materials not by comparison with reference laboratory spectra but using, as reference, spectral shapes exhibited by selected pixels on the scene, whose actual composition is independently (for instance by field observations) known (fig. 4b).

4. Application of the proposed method on a test-area

The proposed method was applied to identify serpentinite outcrops in a topographically complex area of the Pollino National Park. The area is geologically characterised by ophiolitic rocks, Meso-cenozoic platform units and Plio-quaternary sediments (Monaco *et al.*, 1995; Schiattarella, 1996). For this area a detailed geological survey together with a 1:50 000-scale map were available. Among ophiolitic rocks, serpentinite was chosen as a test-rock because it is present in isolated outcrops in the test-area, besides subtending important environmental problems as it contains asbestos.

Before describing, step by step, the application procedure, some aspects must be pointed out:

– The e.m. radiation, detected by airborne sensors operating in the optical range, transports information related only to the Earth surface *skin* (from 50 μm up to few centimetres of depth moving from the VIS to the TIR spectral range). This means that rocks covered by vegetation cannot be detected and identified. For this reason, a vegetation mask was generated to restrict the

following image processing steps only on areas with well outcropping rocks.

– Rocks to be identified can be under different illumination conditions (fig. 5): this possibility was considered choosing supervised classification algorithms less affected by these effects (as the above mentioned SAM working on the shapes of the spectra).

– Each ground pixel can be composed by mixing distinct materials (different kinds of rocks, soil, vegetation, etc.): this circumstance was considered when the possibility to estimate rocky outcrops boundaries was verified.

All 102 MIVIS channels, except noisy bands (at 2.234 μm, 2.265 μm, 2.411 to 2.474 μm), were processed and used in the following steps.

4.1. *Step 1: vegetation mask generation*

Vegetated areas were excluded from the following processing steps by generating a vegetation mask on the basis of spectral signatures, specific to the vegetated surfaces, in the available VIS and TIR MIVIS channels: the MIVIS bands ratio, channel 6/channel 13 (*i.e.* 0.542 μm/0.682 μm), is known to be generally higher whereas the radiant temperature in channel 93 (8.37 μm) is expected systematically lower for vegetated pixels compared with non-vegetated areas. To discriminate non-vegetated areas and, notwithstanding substantial agreement (fig. 6a,b) between the two different tests, the most restrictive solution (radiant temperature test) was chosen and applied to the whole scene to detect

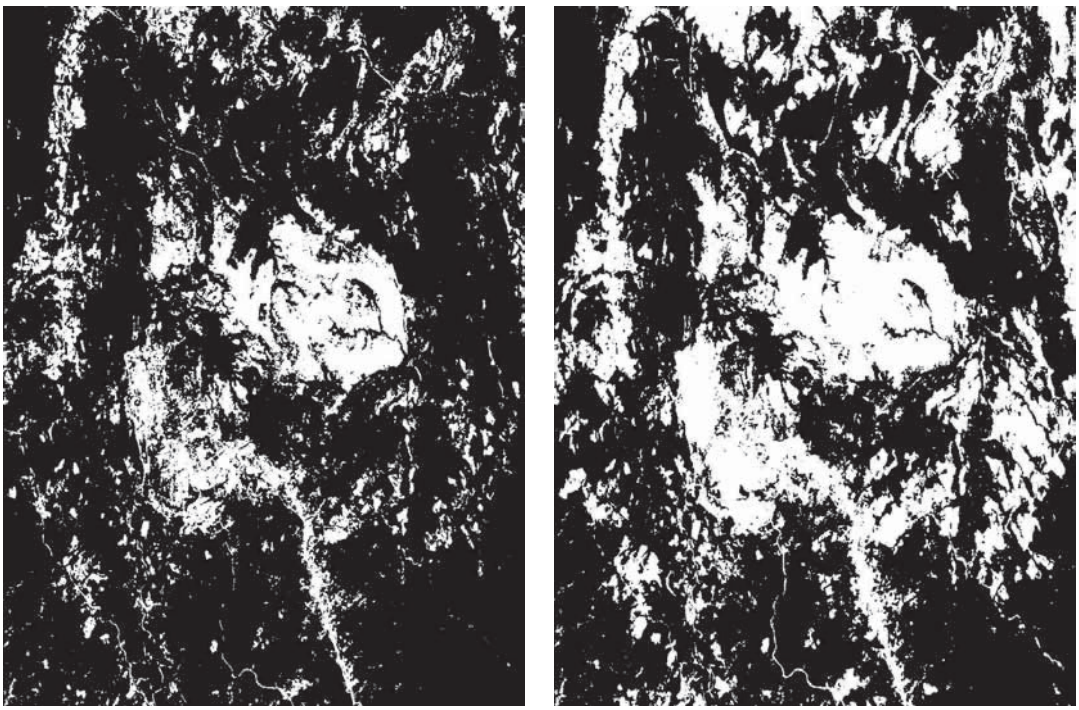

ⓐ ⓑ

Fig. 6a,b. Vegetation masks (S. Severino area) obtained considering: a) MIVIS radiant temperature in channel 93 (8.37 μm) not greater than 303 K; b) bands ratio 6/13 (0.542 μm/0.682 μm) greater than 1.3. Vegetated areas are black, the non-vegetated ones are white (see text).

«well exposed areas» to be retained for the following steps.

4.2. *Step 2: reference radiance spectra selection*

Supervised processing techniques, used in the following steps for rocky outcrops identification as well as for the evaluation of outcrops boundaries, require spectral curves to be used as reference for the materials to be identified on the scene. For this purpose, on the basis of geological maps and aerial photos, limited areas, representative of different materials, were identified on the scene and the corresponding mean spectral radiances (obtained by averaging MIVIS radiances at the sensor for each area) were used, instead of laboratory spectra, as reference (in fig. 7a, for instance, the region of interest chosen for serpentinite is indicated).

4.3. *Step 3: serpentinite identification*

To identify serpentinite outcrops, a supervised classification was used. Such a technique identifies in a scene pixels which have radiance spectra the most similar to the ones exhibited by selected pixels assumed as reference. Identification is made by rules which differ depending on the chosen method. In particular, to identify serpentinite outcrops in

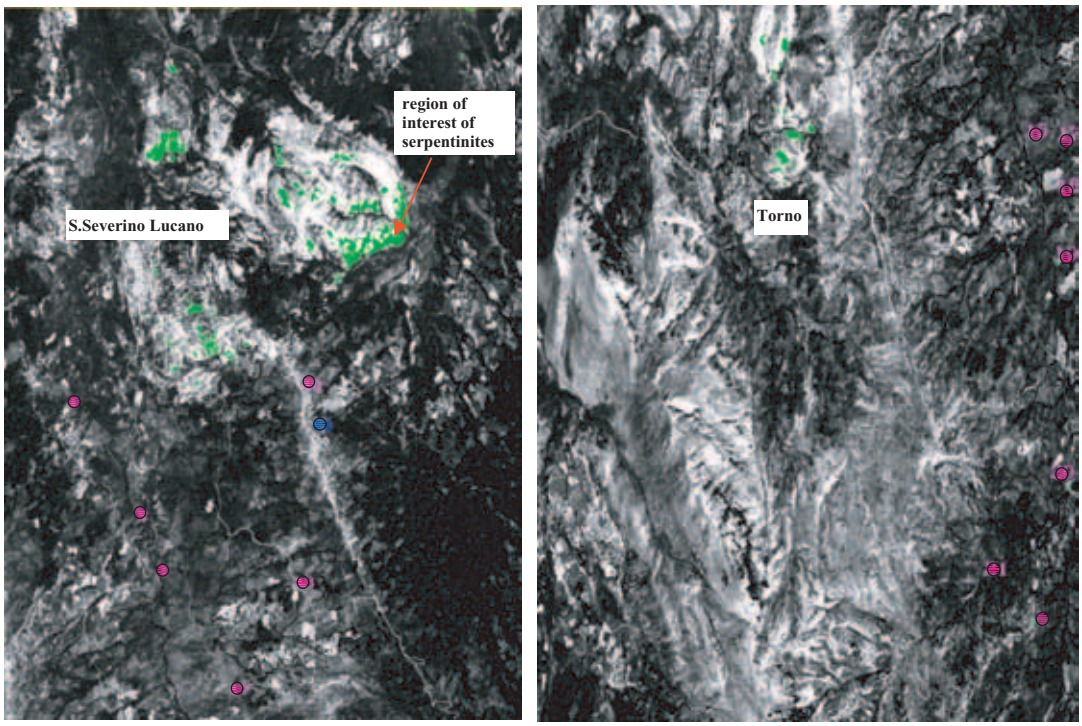

Fig. 7a,b. SAM results corresponding to some zones of the test-area: S. Severino area (a) and the Torno outcrop (b). Serpentinite identified by SAM is indicated in green. Small circles, indicated in different colors, point out isolated pixels corresponding to unmapped serpentinite identified by SAM. The blue circle indicates the site where the photo shown in fig. 9a was taken during the field check.

observational conditions which can be variable across the scene, the SAM method (Kruse *et al*., 1993) was chosen. Working on spectral shapes (instead than on absolute values) the SAM classifier is expected to be less affected by the variable contributions of illumination, topographic and atmospheric effects across the scene.

In particular, SAM considers the angle ϑ between the N-dimensional vector $\boldsymbol{R} \equiv (R_1, R_2, R_3, ..., R_N)$ associated with the reference radiance spectra (being R_i the radiance measured in the band $\Delta\lambda_i$ and N the total number of bands) and the one, $\boldsymbol{r} \equiv (r_1, r_2, r_3, ..., r_N)$, measured at the pixel on the scene to be identified

$$\partial = \arccos\left(\frac{\boldsymbol{R}\cdot\boldsymbol{r}}{R\cdot r}\right) =$$

$$= \arccos\left[\frac{R_1 r_1 + R_2 r_2 + ... + R_N r_N}{\left(R_1^2 + R_2^2 + ... + R_N^2\right)^{\frac{1}{2}}\left(r_1^2 + r_2^2 + ... + r_N^2\right)^{\frac{1}{2}}}\right]$$

The smaller are the θ angles, the closer the resemblance to the reference spectrum. Pixels further away than a specified maximum angle threshold θ_{MAX} are identified as not belonging to the class of materials identified by the specific reference spectral curve $\boldsymbol{R}$. In our case, the MIVIS reference spectrum $\boldsymbol{R}$ for serpentinite (plotted in fig. 2b) was chosen in the well exposed zone of *Timpa della Guardia* (shown in fig. 7a) and the SAM classifier applied to the whole study area using a strong cut with $\theta_{MAX} = 0.1$ rad.

4.4. *Step 4: Rocky outcrops boundaries evaluation*

The possibility to estimate rocky outcrops boundaries was verified, combining SAM and LSU (Linear Spectral Unmixing; Adams *et al*., 1989). The latter is a technique which attempts to model the observed spectral radiance r_i as a mixture of representative «prototype» spectra (*end-members*) as given below

$$r_i = F_j \cdot R_{ij} + \varepsilon_i \qquad \text{with} \qquad \sum_j F_j = 1$$

where r_i denotes the measured radiance of the mixed spectrum in band i, R_{ij} is the radiance in the same band expected for the end member j, F_j is the fraction of material j in the mixture and ε_i is the residual error on r_i.

LSU was applied to define boundaries of serpentinite outcrops, where serpentinite presence was already identified by SAM.

We will discuss here, in particular, the case of the Torno outcrop because its outcropping conditions (vegetated hillside without visible reference points) made it difficult to accurately delimit its boundaries even by direct field observations. In the selected area dominant materials were limestones, serpentinites and vegetation. So their reference spectra were considered as end members to be used in LSU. They have been defined in step 2 and are represented (in the range 0.4-2.5 μm) in Fig. 2b.

5. Results

In order to verify SAM results, MIVIS imagery and image processing products were preliminarily co-registered upon available digital geological maps of the investigated area. *In situ* observations were moreover performed where serpentinite outcrops identified by SAM were not documented elsewhere.

Figure 7a,b shows SAM results in two zones, S. Severino area (a) and the Torno outcrop (b), of the test-area: pixels recognized as serpentinite-made are green. All the small circles, indicated in different colors, emphasize isolated pixels (otherwise not easily visible on the image) identified as serpentinite.They were all checked in field and a photo was taken in the site indicated by the blue circle in fig. 7a and reported in fig. 9a.

SAM results were overlaid on geological maps: fig. 8 shows two examples of that. Pixels recognized as serpentinites by SAM are red coloured.

The overlaying of SAM results over geological maps shows that wherever SAM identifies serpentinite it is really present. In particular, the identification takes place where:

• serpentinite outcrops as bodies which are also pointed out in geological maps (90% of

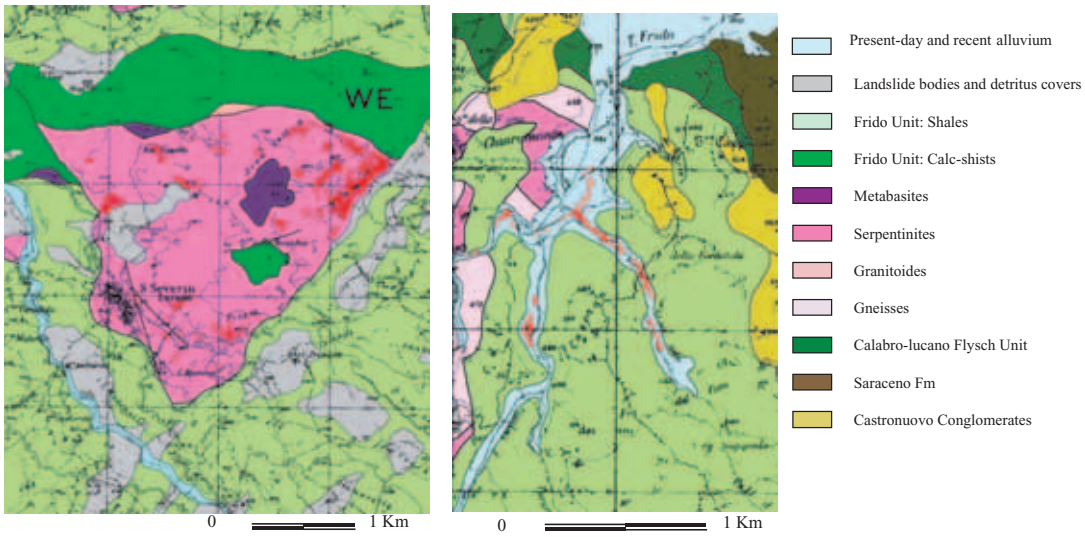

Fig. 8. Serpentinite identified by SAM (red), laid on geological map of S. Severino area (left) and Frido stream (right).

Fig. 9a,b. Some photos showing unmapped serpentinite grounds identified by the proposed method. Left: serpentinite ground along a country road crossing geologically different grounds; right: serpentinite used as road-bed.

«well exposed» outcrops in the test-area were identified by SAM);

• it is present as serpentinite soils which are not mapped elsewhere. Field check (fig. 9a,b) has shown that such serpentinite soils:

– correspond to landslide bodies or alluvial grounds;

– are present, because of man's action, along country roads crossing geologically different grounds;

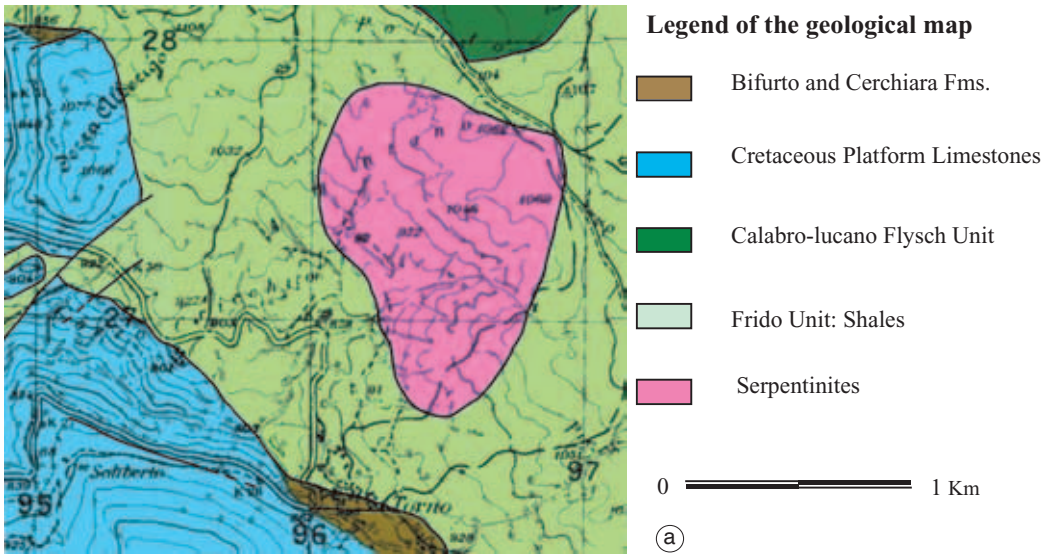

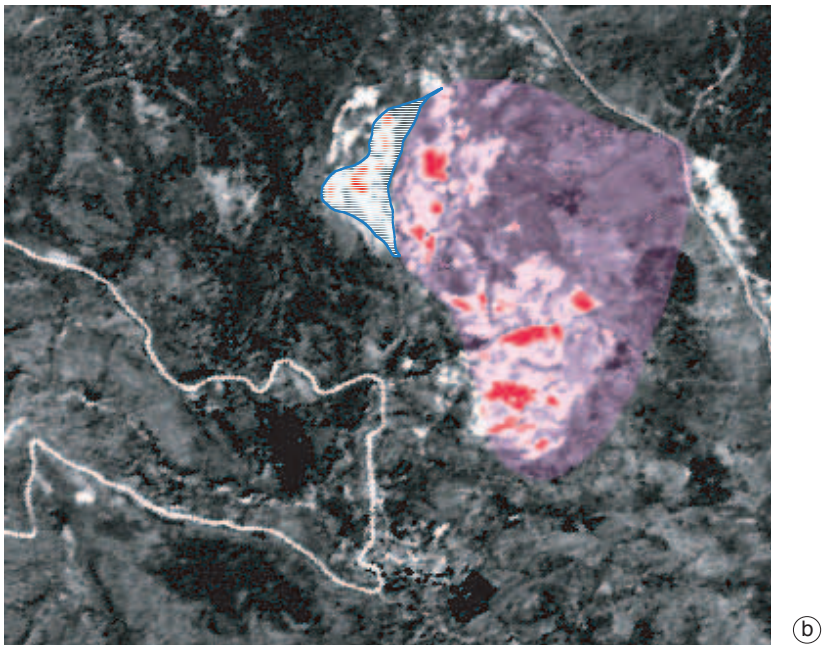

Fig. 10a,b. Outcrop boundaries definition by combined use of SAM and LSU (see text): a) geological map of the area around Torno with serpentinites outcrop boundaries as recognized during field geological survey; b) result of LSU analysis. Grey tones represent different levels, from low (dark) to higher (bright), of serpentinite contributions. Pixels already recognized as serpentinite-made by SAM are coloured in red. The new identified boundaries are indicated in light-blue by comparison with the previously ones (pink).

– are present, because of gravity action, along roads below serpentinite outcrops.

SAM was able to locate serpentinite outcrops, but not to determine their true extension. This happens because of vegetation (which masks the signal leaving the underlying soil), but also because of the presence of mixed pixels whose spectral response is, as already pointed out, the result of the mixing of the contribution of many materials (not exclusively serpentinite). The less is the serpentinite contribution in each mixed pixel, the more the similarity between the pure serpentinite spectral end member and the observed spectra decreases. As a result, SAM does not identify that such pixels also contain serpentinite. The combined use of SAM and LSU estimated selected outcrop boundaries.

Figure 10a,b shows the combined use of SAM and LSU analysis in the case of the Torno serpentinite outcrop. Figure 10a shows the geological map of the area around Torno with serpentinites outcrop boundaries as recognized, or simply inferred, during field geological survey. Such boundaries are reported, as a pink transparency, also in fig. 10b where pixels recognized by SAM as serpentinite-made are coloured in red. The underlying grey-tone image in fig. 10b is the result of LSU analysis performed using only three end-members corresponding to the dominant surface material (vegetation, limestones and serpentinites) present in the Torno area. Grey tones represent different levels, from low (dark) to higher (bright), of serpentinite contributions. Such interpretation remains valid wherever the mixing of surface materials includes the ones considered for the Torno area and not where the presence of other materials (not included as end-members in the LSU processing) can make such an interpretation misleading (see for example as even asphalt roads appear bright in fig. 10b). Starting from this consideration, it is correct to suppose that at least white pixels around the red ones (already recognized as serpentinite by SAM) have a really high probability of being dominated by the presence of serpentinite in concurrence of lower percentages of vegetation and limestones. In this way, considering the combination between SAM and LSU results, it is possible to give evidence of an underestimation of the outcrop extension whose northern boundary has to be moved to NW with respect to boundaries derived from field geological survey (fig. 10b).

In conclusion:

• test-rock identification by SAM shows:

– starting from field information relative to small areas (reference outcrops), it is possible to locate the same rock within a rather wide area, pointing out hyperspectral data possibility in searching any material within a wide area of distribution;

– possibility to identify test-rock along riverbeds, which can be important in detecting a particular material within alluvial ground;

– the proposed technique can be used to locate materials containing polluting substances (serpentinite contains asbestos).

• the combined use of LSU and SAM shows that such a methodology could be helpful in geological mapping when ground conditions do not allow an easy survey.

• the proposed methodology can be exported to any kind of material, any geographical area (even with complex orography) and independently on the availability of coincident information on atmospheric parameters, as no atmospheric or topographic correction are required.

Acknowledgements

This work was carried out within the framework of the «Progetto Pollino» (POP-FESR 1994-96), funded by European Economic Community and Regione Basilicata.

REFERENCES

ADAMS, J.B., M.O. SMITH and A.R. GILLESPIE (1989): Simple models for complex natural surfaces: a strategy for the hyperspectral era of remote sensing, in *Proceeding of the IGARSS '89 Symposium*, *July 10-14*, *Vancouver*, *Canada*, 16-21.

BEN-DOR, E., F.A. KRUSE, A.B. LEFKOFF and A. BANIN (1994): Comparison of 3 calibration techniques for utilisation of GER 63-channel aircraft scanner data of Makhtesh-Ramon, Negev, Israel, *Photogramm. Eng. Remote Sensing*, **60**, 1339-1354.

BIANCHI, R., C.M. MARINO and S. PIGNATTI (1994): Airborne hyperspectral remote sensing in Italy, in *Proceedings EUROPTO series «Recent Advances in*

Remote Sensing and Hyperspectral Remote Sensing» SPIE Roma, 27-29 September 1994, **2318**, 29-37.

CLARK, R.N., T.V.V. KING, M. KLEJWA, G.A. SWAYZE and N. VERGO (1990): High spectral resolution reflectance spectroscopy of minerals, *J. Geophys. Res.*, **95**, 12,653-12,680.

CLARK, R.N., G.A. SWAYZE, K. HEIDEBRECHT, R.O. GREEN and A.F.H. GOETZ (1995): Calibration to ground reflectance of terrestrial imaging spectroscopy data: comparison of methods, in *Proceeding of the 5th Annual JPL Airborne Geoscience Workshop, JPL publication 95-1* (Pasadena, CA: Jet Propulsion Laboratory), 41-42.

CUOMO, V., N. AFFLITTO, M. BLUMETTI, A. BONFIGLIO, O. CANDELA, T. CARONE, G. DI BELLO, C. FILIZZOLA, T. LACAVA, A. LANORTE, V. LANORTE, R. LASAPONARA, M. MACCHIATO, L. MINERVINI, F. MUNDO, N. PERGOLA, C. PIETRAPERTOSA, S. PIGNATTI, E. ROMANO, T. SIMONIELLO, V. TRAMUTOLI and A. ZACCAGNINO (2001): Pollino Project Action D: A multi-scale approach, in the space-time domain, to environmental risk monitoring, in *Remote Sensing for Environmental Monitoring, GIS Applications and Geology*, edited by M. EHLERS, E. ZILIOLI and H.J. KAUFMANN, *Proceedings of SPIE* 4545-02.

FARRAND, W.H., R.B. SINGER and E. MERENYI (1994): Retrieval of apparent surface reflectance from AVIRIS data – a comparison of empirical line, radiative-transfer and spectral mixture methods. *Remote Sensing Environ.*, **47**, 311-321.

KRUSE, F.A., A.B. LEFKOFF, J.B. BOARDMAN, K.B. HEIDEBRECHT, A.T. SHAPIRO, P.J. BARLOON and A.F.H. GOETZ (1993): The Spectral Image Processing System (SIPS)-Interactive visualization and analysis of imaging spectrometer data, *Remote Sensing Environ.*, **44**, 145-163.

MCARDLE, S.S., J.R. MILLER and J.R. FREEMANTLE (1992): Airborne image acquisition under cloud: preliminary comparisons with clear-sky scene radiance and reflectance imagery, in *Proceedings of the 15th Canadian Symposium on Remote Sensing* (Toronto: Canadian Remote Sensing Society & Canadian Aeronautics and Space Institute), 446-449.

MONACO, C., L. TORTORICI, L. MORTEN, S. CRITELLI and C. TANSI (1995): Geologia del versante nord-orientale del massiccio del Pollino (confine calabro-lucano): nota illustrativa sintetica della Carta geologica alla scala 1:50.000. *Boll. Soc. Geol. It.,* **114**, 277-291.

SALISBURY, J.W. and D.M. D'ARIA (1992): Emissivity of terrestrial materials in the 8-14 μm atmospheric window. *Remote Sensing Environ.*, **42**, 83-106.

SCHIATTARELLA, M. (1996): Tettonica della Catena del Pollino (Confine calabro-lucano). *Mem. Soc. Geol. It.*, **51**, 543-566.

SMITH, G.M. and E.J. MILTON (1999): The use of the empirical line method to calibrate remotely sensed data to reflectance, *Int. J. Remote Sensing*, **20**, 2653-2662.